Ladder Climbing on the Anharmonic Intermolecular Potential in an Amino Acid Microcrystal via an Intense Monocycle Terahertz Pulse

Mukesh Jewariya,[1,2] Masaya Nagai,[1,3,*] and Koichiro Tanaka[1,2,4]

[1]*Department of Physics, Kyoto University, Kyoto 606-8502, Japan*
[2]*Core Research for Evolutional Science and Technology, Japan Science and Technology Agency, Japan*
[3]*Precursory Research for Embryonic Science and Technology, Japan Science and Technology Agency, Japan*
[4]*Institute for Integrated Cell-Material Sciences, Kyoto University, Kyoto 606-8501, Japan*

(Received 1 June 2010; published 11 November 2010)

We experimentally demonstrated 20 ladder climbing steps on the anharmonic intermolecular potential in the amino-acid microcrystals with an intense monocycle terahertz pulse. Absorption spectra show the suppression of the peak and enhancement of the low-frequency absorption for the incident electric field amplitude. These results are reproduced by simulations based on coherent transition processes between quantum levels in the anharmonic potential. The appearance of such nonlinearity allows us to control macroscopic motion via a phase-controlled terahertz pulse.

DOI: 10.1103/PhysRevLett.105.203003 PACS numbers: 33.20.Xx, 33.20.Ea, 78.47.jh

Ultrashort optical pulse excitations for molecules and solids have attracted interest from the viewpoint of the novel efficiency control of chemical reactions and macroscopic phase transitions. Optical excitation into an electric excited state often causes molecular dissociation or transformation, which opens a pathway for synthesizing new structures and materials [1–4]. An alternative method is a direct vibrational excitation of the reaction mode by intense infrared ultrashort pulses. Cascading transitions from the ground state to higher vibrational states through a series of intermediate levels may allow us to reach the critical condition for the transformation of molecular or crystal structure [5], which is usually referred to as ladder climbing. It is classically equivalent to large-amplitude motion driven by intense force applied over a shorter time than the vibration period. Since the vibrational mode is essentially anharmonic, a chirped pulse excitation is promising for efficient excitation. Many researchers have succeeded climbing a few stairs [6–10].

Molecular or ionic motion in the terahertz (THz) frequency region are also attractive because they are decisive for the macroscopic properties of solids, such as ferroelectricity or ferroelasticity. There are several reports on large-amplitude THz motion driven by an optical ultrashort pulse through impulsive stimulated Raman scattering (ISRS). Controlled access to anharmonic regions of lattice potential energy surfaces was demonstrated for the soft mode [11]. The softening of the coherent phonon mode has been reported in bismuth, which shows the precursor of a new photo-induced phase transition [12]. In flexible macromolecules, low-frequency motions often govern the conformational transformation, and nonlinear signals are observed in heme protein [13]. These motions are essentially limited only for the Raman-active mode. Here, we focus on the direct excitation of anharmonic IR-active vibration with intense THz monocycle pulse excitation that can induce extremely large-amplitude motions via ladder climbing processes. Excitation efficiency should be much higher than that of ISRS. The IR-active mode is more relevant to the chemical reaction or structural change. Xie *et al.* performed THz pump-probe measurements in bacteriorhodopsin using a free electron laser, and a nonlinear signal has been reported for the first time [14]. Even in ferroelectric materials, new domain orientation control with a THz pulse has been proposed [15]. However, nonlinearity of the bosonic vibration mode is intrinsically less apparent than the fermionic electron system, which has difficulties in its observation of nonlinear responses. Recently, intense THz pulse generation has been demonstrated using a tilted pulse-front optical pulse and a high-$\chi^{(2)}$ $LiNbO_3$ crystal [16], with which significant nonlinear signals have been reported in dielectric materials even in the nonresonant region[17]. In this paper, we report the nonlinear responses of amino-acid microcrystalline powder pellets using an intense monocycle THz pulse. The field amplitude dependence of transmission spectra shows clear anharmonicity of intermolecular vibrations, and ladder climbing above ten steps is successfully made on the anharmonic intermolecular potential.

We measured *L*-arginine (Wako Pure Chemical Industries Ltd.) powder in a polythene matrix pellet. We mixed 30 mg of arginine microcrystals, with a grain size of several tens μm, with polythene powder at a ratio of 1:5 and pressed into a 1 mm-thick pellet. Figure 1 shows the absorption spectra of an *L*-arginine pellet at different temperatures using the THz linear spectroscopy system. One can see a sharp absorption peak at 1.1 THz and an absorption tail in the high frequency region at 13 K. Since these absorption peaks disappear completely in the solution, we assign them as intermolecular vibration modes in the microcrystal. These absorptions become broadened monotonically towards the low-frequency region with

increasing temperature. This behavior is different from that of sugar, where a complicated spectral shift appears by changing the temperature [18]. Korter *et al.* pointed out that the monotonically low-frequency spectral shift of the intermolecular vibration mode allows us to approximate the simplest anharmonic potential, the Morse potential, for intermolecular vibration [19]. A schematic diagram is shown in the inset of Fig. 1. The transition frequency between n and $n+1$ quantum levels in the potential can be approximated as $\nu_{n,n+1} = \nu_0\ [1 - 2\chi(n+1)]$ in the case of small n and χ, where ν_0 and χ are the resonance frequency at low temperature and the anharmonic parameter, respectively. The resonance frequency of the transition $\nu_{n,n+1}$ shifts toward the low-frequency side with a discrete energy interval of $2\chi\nu_0$ as n increases. The spectral line shape of each transition with the line width $\Delta\nu$ is given by $\gamma(\nu - \nu_{n,n+1})$, and the absorption coefficient is described as $\alpha(\nu) \propto \nu\sum_{i=0}\{\mu^2_{i,i+1}(N_i - N_{i+1})\gamma(\nu - \nu_{i,i+1})\}$, where $N_n - N_{n+1}$ is the difference of the thermally distributed populations. We used the dipole moment matrix $\mu^2_{n,n+1} = \mu^2_0(n+1)(1-2\chi n)$ for the Morse potential with a second-order perturbation [20]. We determined ν_0 and χ from the peak positions at 13 K and 300 K. We evaluated $\gamma(\nu)$ from the spectrum at 300 K as the Gaussian function, with the assumption that the inhomogeneous broadening is dominant. The calculated absorption spectrum at 300 K is shown as a dashed curve in Fig. 1. We assume two intermolecular vibration modes, a and b, and a scattering component ($\propto \nu^4$). Prominent features of the spectra are almost reproduced, even using a simple model.

In the experiment, we used optical pulses from an amplified Ti:sapphire laser system (1 kHz, 580 mW, 780 nm, 150 fs). The beam is split into two beams, one for THz pulse generation and another for electro-optical sampling. The excitation beam with a tilted pulse front, controlled by using a grating and a lens pair, is incident on the Mg doped (1.5%) $LiNbO_3$ prism as an emitter. The emitted THz pulse is focused on the sample and electro-optic crystal. We obtain a time profile of the electric field by varying the time delay between the probe and THz beams and the Fourier-transformed optical density and relative phase spectra are evaluated from temporal waveforms with and without the sample. If we change the input power of the optical pump pulse for a changing THz field amplitude, the profile of the THz pulse is strongly distorted due to a cascaded $\chi^{(2)}$ process [21,22]. Thus, we used a set of two wire-grid polarizer (Murata Manufacturing Co., Ltd., EWG20-1M) pairs as variable attenuators. We have carefully checked the profile of the THz electric field, maintained up to 1/32 amplitude attenuation.

Figure 2 shows the optical density spectra at different amplitudes of an incident THz pulse. The upper part shows the power spectrum of the incident THz pulse that passes with or without the sample. The inset shows the temporal profile of the THz electric field on the sample position. The maximum electric field approaches 100 kV/cm [21]. With an increasing incident field amplitude, the absorption peak gradually reduces and, alternatively, the optical density below 0.4 THz increases. While the phase information is useful for the analysis of two-level Rabi oscillation [23], we observe little phase change. This preferably allows simple spectral analysis without a self-focusing effect. Closed circles in Fig. 3 show the optical density at 1.0 THz as a function of the incident electric field amplitude. The bottom axis in this plot shows the relative amplitude of the incident electric field for later discussions, and $E/E_{\max} = 1$ corresponds to the THz pulse with a maximum field of 100 kV/cm. Below the maximum

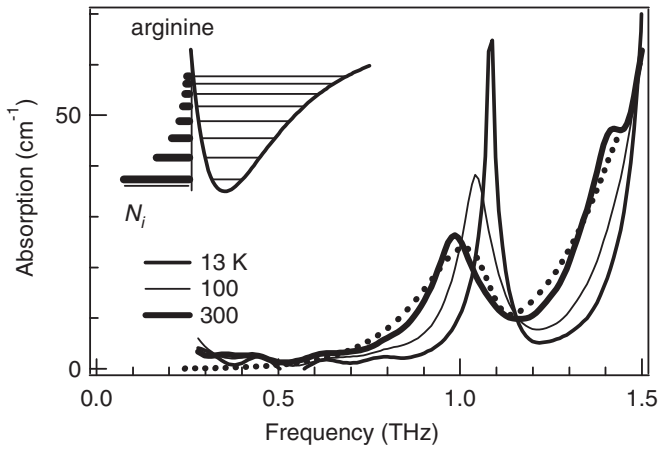

FIG. 1. Absorption spectra of an L-arginine pellet at 13, 100, and 300 K. We show the simulated spectrum at 300 K as a dashed line. The inset shows the approximated potential shape for the intermolecular vibration mode. In this simulation we assume two nonlinear oscillators, a and b, with the parameters $\nu^{(a)}{}_0 = 1.09$ THz, $\nu^{(b)}{}_0 = 1.59$ THz, $\chi^{(a)} = 0.008$, $\chi^{(b)} = 0.008$, $\mu^{(b)} = 1.4\mu^{(a)}$, $\Delta\upsilon^{(a)} = 0.1$ THz, and $\Delta\upsilon^{(b)} = 0.15$ THz.

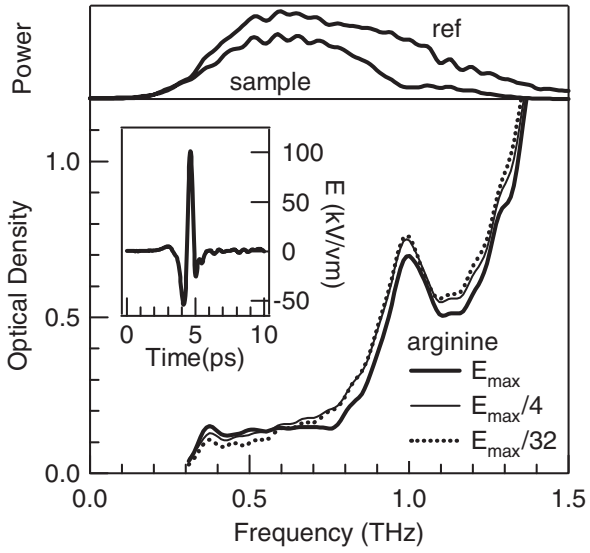

FIG. 2. Optical density of an L-arginine pellet at different incident amplitudes of THz pulses. The inset shows the incident THz pulse. The upper part shows the power spectra of the THz pulse passing through the sample and without the sample.

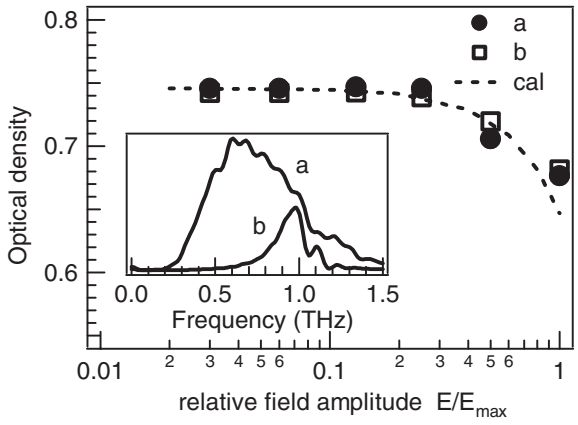

FIG. 3. The incident electric field amplitude dependence of the optical density at 1 THz. The dashed curve shows the simulated optical density if we assume $\mu^{(a)}{}_0 E_0/h = 0.9$ ps is equivalent to that at 100 kV/cm. The inset shows the power spectra of the incident THz pulse with and without the bandpass filter.

electric field of 25 kV/cm, the optical density does not change, and it decreases above this electric field. These results clearly show nonlinear behaviors.

We expect the large-amplitude intermolecular vibration coherently driven by the intense THz pulse to cause nonlinearity. The observed spectra are slightly different from the linear spectrum at high temperatures, but the spectral weight shift toward the low-frequency region shows the characteristic feature of anharmonicity for the intermolecular vibration mode. One of the most likely interpretations is the polarization change via the rearranged mode population. Since this rearranged population in the multilevel system is far from an inverse population providing phase-shifted reemission, analysis of the optical density change is useful.

We verify specific frequency components clearly contributing to resonant nonlinear responses with the control of the incident excitation pulse profile, because the classical field amplitude is more decisive for phenomena under an intense ac field in an electric system [24]. We inserted a 1.0 THz bandpass filter (Murata Manufacturing Co., Ltd., MMBPF40-1000) before the sample. The inset of Fig. 3 shows the power spectra of the THz pulse with and without a bandpass filter. The Fourier component at 1.0 THz is maintained even with the filter, while the maximum amplitude of the electric field is strongly attenuated (40%) with the filter. We add the optical density at 1.0 THz with a narrow band excitation, shown as open squares in Fig. 3. The bottom axis corresponds to the Fourier amplitude at 1.0 THz in this case. We add a 0.08 offset to it in this plot, because the finite time span limited by multireflection reduces the optical density. The saturation of the peak absorption is apparent, with the same relative amplitude of the incident THz electric field. This supports the fact that the resonant components are decisive for the observed nonlinearity.

There are many classical theories for anharmonic oscillators, which is useful for the analysis of the nonlinear response in a liquid [25,26]. Since the oscillator has anharmonicity in the presence of a heat bath, the interaction of normal modes with their environment strongly influences the broadened spectral line shape. However, the absorption shape in our sample is asymmetric on the low-frequency side, as shown in Fig. 1, and we expect longer dephasing time than THz pulse duration. Therefore, we assume that the spectral change is mainly attributed to large-amplitude impulsive motion before energy dissipation, and we evaluate the spectral shape with the assumption of the coherent transition process in several quantum levels in the anharmonic potential. Since the temporal evolution of the density matrix driven by the monocycle field can be easily calculated in a two-level system [27,28], we extend this model to a system of several energy levels. Assuming an ith energy level, differential equations of the density matrix $\rho_{i,j}$ are expressed as follows

$$\frac{d\rho_{i,i}(t)}{dt} = -\gamma_1(\rho_{i,i} - \rho_{i+1,i+1}) - i\frac{E(t)}{\hbar}(\mu_{i-1,i}\rho_{i,i-1} - \mu^*_{i-1,i}\rho^*_{i,i-1}) + i\frac{E(t)}{\hbar}(\mu_{i,i+1}\rho_{i+1,i} - \mu^*_{i,i+1}\rho^*_{i+1,i}), \quad (1)$$

$$\frac{d\rho_{i+1,i}(t)}{dt} = \frac{d\rho^*_{i,i+1}(t)}{dt} = -\left(i2\pi\nu_{i,i+1} + i(\mu_{i+1,i+1} - \mu_{i,i})\frac{E(t)}{\hbar} + \gamma_2\right) \times \rho_{i+1,i} - i\frac{E(t)}{\hbar}\mu_{i+1,i}(\rho_{i+1,i+1} - \rho_{i,i}), \quad (2)$$

where γ_1 and γ_2 are longitudinal and transverse relaxation rates. We assume that the linewidth of each transition in the linear spectra is dominantly determined by γ_2, so we set $\gamma_1 = 0$ and $\gamma_2 = \pi\Delta\nu$. We neglect the dipole moment difference $\mu_{i+1,i+1} - \mu_{i,i} = 0$. As an initial condition of the density matrices, we assume that the diagonal components $\rho_{ii}(0)$ obey Maxwell-Boltzmann distribution at room temperature, and off-diagonal components are zero $[\rho_{i,i+1}(0) = 0]$. The incident electric field profile is approximated as $E(t) = E_0 \exp[-(t/\tau)^2]\cos\Omega t$, where $\Omega/2\pi = 0.7$ THz and $\tau = 0.5$ ps. Thus, we calculate the temporal evaluation of the polarization described by the off-diagonal density matrix $P(t) = \mathrm{Tr}[\mu\rho]$. For simplification, we use the attenuation spectra from Fourier-transformed $\mathrm{Im}[\nu P/E]$. P/E, in the low electric field limit, corresponds to electric susceptibility, which bring in the attenuation coefficient $\mathrm{Im}[\nu P/E]$, with the approximation of the refractive index unchanged in all frequency regions [27]. This is proportional to the absorption spectra in Fig. 1.

Figure 4(b) shows the time evolution of the polarizations. The incident field amplitudes are $\mu_0 E_0/h = 0.02$ and 1 ps^{-1}, respectively, and the profiles are normalized by the incident electric field amplitude E_0. One can see that the shape of the polarization profile changes with a large

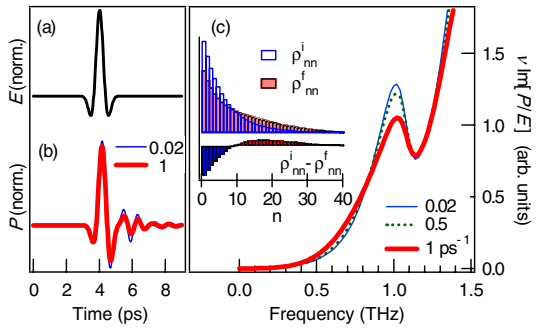

FIG. 4 (color online). Time profile of (a) the incident electric field and (b) polarization. (c) Fourier-transformed $\nu P/E$ with different incident electric fields of $\mu^{(a)}{}_0 E_0/h = 0.02$, 0.5, and 1 ps^{-1}. The inset shows the initial and final mode populations $\rho^{i,f}{}_{nn}$ and change $\Delta\rho^{(a)}{}_{nn}$ after the maximum field injection.

incident electric field amplitude. Figure 4(c) shows the corresponding attenuation spectra $\nu P/E$ at different incident field amplitudes. Absorption above 0.8 THz is saturated, and the low-frequency tail of the 1.5 THz absorption peak is also reduced. Coincidently, the low-frequency absorption increases. Prominent features of the simulated spectra are almost reproduced by the experimental results, even using a simple approximation. Therefore, we conclude that an intense monocycle THz pulse excitation brings about a large-amplitude vibration mode, and the polarization may be changed due to the rearrangement of the vibrational population at quantum levels of the anharmonic potential.

We add the absorption peak at different values of $\mu^{(a)}{}_0 E_0/h$, shown as the dashed curve in Fig. 3. The calculated absorption is slightly smaller than experimental results as shown in Fig. 1, so we compensate simulated values of optical density in Fig. 3. From the simulated spectra at $\mu^{(a)}{}_0 E_0/h = 0.8\,\mathrm{ps}^{-1}$, similar to those at the 100 kV/cm maximum electric field, we evaluate the dipole moment of the intermolecular vibration $\mu^{(a)}{}_0 = 5e\mathring{\mathrm{A}}$.

The evaluated diagonal components $\rho_{n,n}$ show the mode population, while the off-diagonal components show the polarization. The lower part of Fig. 4(c) shows the change of $\rho_{n,n}$ at the maximum field amplitude. The mode population around the levels with $\langle n\rangle = 2.2$ rises to a higher level with $\langle n\rangle = 22.2$, indicating ladder climbing of 20 steps. This is far from thermal equilibrium.

These simulated results are not completely reproduced by the experimental results. Simulated spectra are strongly sensitive to the temporal shape of the incident electric field. Additionally, the responses are also strongly reflected by the assumed potential shape and quantum levels which are due to numerous collective modes coupling. Conversely, the discrepancy of numerical simulations includes some information on these collective motions. Our work promisingly leads to new THz multidimension spectroscopy which reveals complex mode coupling in a macromolecules system and also reveals a novel THz technique driving collective and functional molecular motion.

The authors acknowledge a Grant-in-Aid for the global COE "The Next Generation of Physics, Spun from Universality and Emergence" and a Grant-in-Aid for Creative Scientific Research (18GS0208), from the Ministry of Education, Culture, Sports, Science, and Technology (MEXT) of Japan. The authors would like to thank I. Katayama for valuable discussions.

*mnagai@scphys.kyoto-u.ac.jp

[1] W. S. Warren, H. Rabitz, and M. Dahleh, Science **259**, 1581 (1993).
[2] R. N. Zare, Science **279**, 1875 (1998).
[3] H. Rabitz *et al.*, Science **288**, 824 (2000).
[4] A. Pashkin *et al.*, Phys. Rev. Lett. **105**, 067001 (2010).
[5] E. R. Grant *et al.*, Phys. Rev. Lett. **40**, 115 (1978).
[6] A. Assion *et al.*, Chem. Phys. Lett. **259**, 488 (1996).
[7] D. J. Mass *et al.*, Chem. Phys. Lett. **290**, 75 (1998).
[8] V. D. Kleiman *et al.*, Chem. Phys. **233**, 207 (1998).
[9] L. Windhorn *et al.*, Chem. Phys. Lett. **357**, 85 (2002).
[10] T. Witte *et al.*, J. Chem. Phys. **118**, 2021 (2003).
[11] C. J. Brennan and K. A. Nelson, J. Chem. Phys. **107**, 9691 (1997).
[12] M. Hase, M. Kitajima, S. Nakashima, and K. Mizoguchi, Phys. Rev. Lett. **88**, 067401 (2002).
[13] F. Rosca *et al.*, J. Phys. Chem. A **106**, 3540 (2002).
[14] A. Xie, A. F. G. Meer, and R. H. Austin, Phys. Rev. Lett. **88**, 018102 (2001).
[15] T. Qi *et al.*, Phys. Rev. Lett. **102**, 247603 (2009).
[16] J. Hebling *et al.*, J. Opt. Soc. Am. B **25**, B6 (2008).
[17] J. Hebling, K.-L. Yeh, M. C. Hoffmann, and Keith A. Nelson, IEEE J. Sel. Top. Quantum Electron. **14**, 345 (2008).
[18] M. Walther, B. M. Fischer, and P. U. Jepsen, Chem. Phys. **288**, 261 (2003).
[19] T. M. Korter and D. F. Plusquellic, Chem. Phys. Lett. **385**, 45 (2004).
[20] B. L. Crawford and H. D. Dinsmore, J. Chem. Phys. **18**, 983 (1950).
[21] M. Jewariya, M. Nagai, and K. Tanaka, J. Opt. Soc. Am. B **26**, A101 (2009).
[22] M. Nagai *et al.*, Opt. Express **17**, 11543 (2009).
[23] C. W. Luo *et al.*, Phys. Rev. Lett. **92**, 047402 (2004).
[24] S. Chelkowski, A. D. Bandrauk, and P. B. Corkum, Phys. Rev. Lett. **65**, 2355 (1990).
[25] K. Okumura and Y. Tanimura, J. Chem. Phys. **105**, 7294 (1996).
[26] U. Häberle and G. Diezemann, J. Chem. Phys. **122**, 184517 (2005).
[27] R. Laudon, *The Quantum Theory of Light* (Oxford University Press, New York, 2000), 3rd ed.
[28] L. W. Casperson, Phys. Rev. A **57**, 609 (1998).